Supporting Information

Chen et al. 10.1073/pnas.0905046106

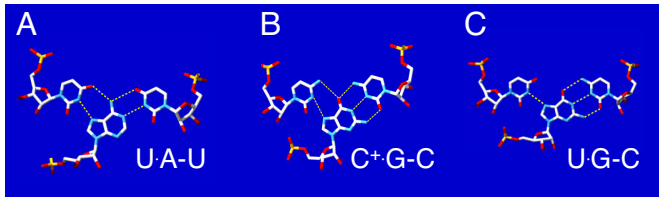

Fig. S1. Structures of major-groove base triples. All of the structures are taken from Non-canonical Base Pair Database (http://prion.bchs.uh.edu/bp_type/) (1). Mutant 102C has higher unfolding force and higher –1 ribosomal frameshifting (FS) efficiency than mutant 101C (45 pN, 33% versus 38 pN, 11%), although each have 1 U·A-U major-groove base triple disrupted (see Figs. 1 and 6). The results suggest that both base stacking and paring interactions are critical for mechanical stability and FS efficiency. During the progress of this work, a refined NMR structure revealed that an extra terminal major-groove base triple (U103·G178-C112) (see *C*) is formed in ΔU177 (*2*). Mutant 102C has the base triple U102·A176-U113 disrupted that destabilizes the stacking with base U101 and may disrupt a less stable base triple (U103·G178-C112) (2), whereas mutant 101C has the base triple U101·A175-U114 disrupted that destabilizes base stacking with the base U100 and base U102. Consistently, previous thermal unfolding studies of DNA triplexes revealed that a terminal base triple is less important than internal ones in thermodynamic stability (3).

1. Nagaswamy U, et al. (2002) NCIR: A database of non-canonical interactions in known RNA structures. *Nucleic Acids Res* 30:395–397.
2. Kim NK, Zhang Q, Zhou J, Theimer CA, Peterson RD, Feigon J (2008) Solution structure and dynamics of the wild-type pseudoknot of human telomerase RNA. *J Mol Biol* 384:1249–1261.
3. Soto AM, Loo J, Marky LA (2002) Energetic contributions for the formation of TAT/TAT, TAT/CGC$^+$, and CGC$^+$/CGC$^+$ base triplet stacks. *J Am Chem Soc* 124:14355–14363.

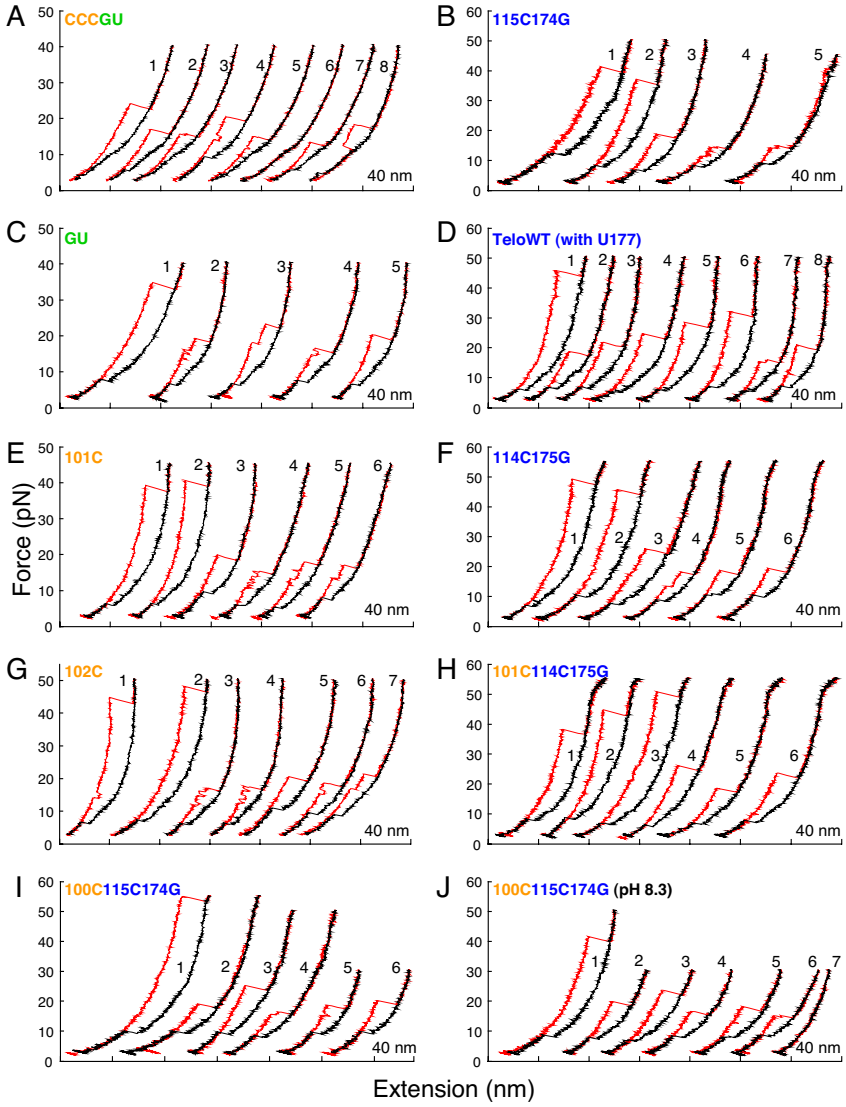

Fig. S2. Representative force-extension curves for the pseudoknots studied here. All pseudoknot mutants were made based on ΔU177 (Figs. 1*B* and 3*C*). Red and black curves are for pulling and relaxing, respectively, with waiting time at approximately 3 pN for 0 or 10 seconds. Folding transitions of stem 1 hairpins were typically observed below 10 pN (see Fig. 2*K*), at which force the folding intermediate structure forms rapidly by partial formation of stem 2 (Fig. 3). By increasing the force above 10 pN, hopping between stem 1 hairpin and the folding intermediate structure was observed with extension change of approximately 5 nm (see Fig. S6 for constant-force trajectories). Hopping becomes less frequent by destabilizing stem 1 hairpin and/or stabilizing stem 2. For example, hopping between stem 1 hairpin and folding intermediate at 10–20 pN is more frequent for ΔU177 (see Fig. 2*B*), mutant GU (*C*, trace 2), mutant 101C (*E*, trace 4), and mutant 102C (*G*, traces 3 and 4) than for the other mutants. Transient formation of folding intermediate structure at approximately 5 pN was observed for a similar pseudoknot with lengthened 12-bp stem 1 and 29-nt loop 2 (1). Thus, shortening of loop 2 and stem 1 increases the intramolecular docking rate to form folding intermediate but does not increase the rate to form native pseudoknot. In *A*, trace 6, stem 1 hairpin is not formed and the plateau at approximately 10 pN with extension change of 2–4 nm is probably due to formation of small non-native hairpin, for example, a 5-bp triloop formed from G107 to C119 (1), which is also present for most of the other force relaxing traces for all of the pseudoknot sequences. In *A*, trace 7, only stem 1 hairpin is formed as indicated by the extension increase of only approximately 11 nm. In *A,* trace 8, folding zipping transition occurred when force was increased. About 5% of all traces for all of the pseudoknot sequences were observed to have only stem 1 hairpin or a small non-native hairpin formed before the force was increased. These traces are not included for analysis as shown in Table S1. The RNA/DNA handle may be partially overstretched (2) with force above 50 pN as seen in panels *B*, *D*, *F*, and *H*. To minimize the RNA/DNA handle artifact and tether-breaking events due to rupture of the digoxigenin-antidigoxigenin interaction, we changed the pulling force range from 3 to >50 pN to 3–30 pN after observing a 1-step high-force (≈50 pN) unfolding event (see *J*). During the force-ramp cycles (3–30 pN), the low-force unfolding and folding transitions were observed as before. However, sometimes no unfolding/folding transition <30 pN or a plateau at approximately 10 pN is present (*J*, trace 7). After resetting the pulling force range to 3 to >50 pN, a high-force 1-step unfolding (≈50 pN) event was again observed. Thus, the absence of unfolding and folding transitions below 30 pN is due to formation of a stable structure—the native pseudoknot, which has a high-force (>40 pN, see Fig. 4*H*) 1-step unfolding transition. Taken together, our results suggest that the high-force and low-force unfolding reactions correspond to native pseudoknot structure and folding intermediate structures (see Fig. 3), respectively.

1. Chen G, Wen J-D, Tinoco I, Jr (2007) Single-molecule mechanical unfolding and folding of a pseudoknot in human telomerase RNA. *RNA* 13:2175–2188.
2. Smith SB, Cui Y, Bustamante C (1996) Overstretching B-DNA: The elastic response of individual double-stranded and single-stranded DNA molecules. *Science* 271:795–799.

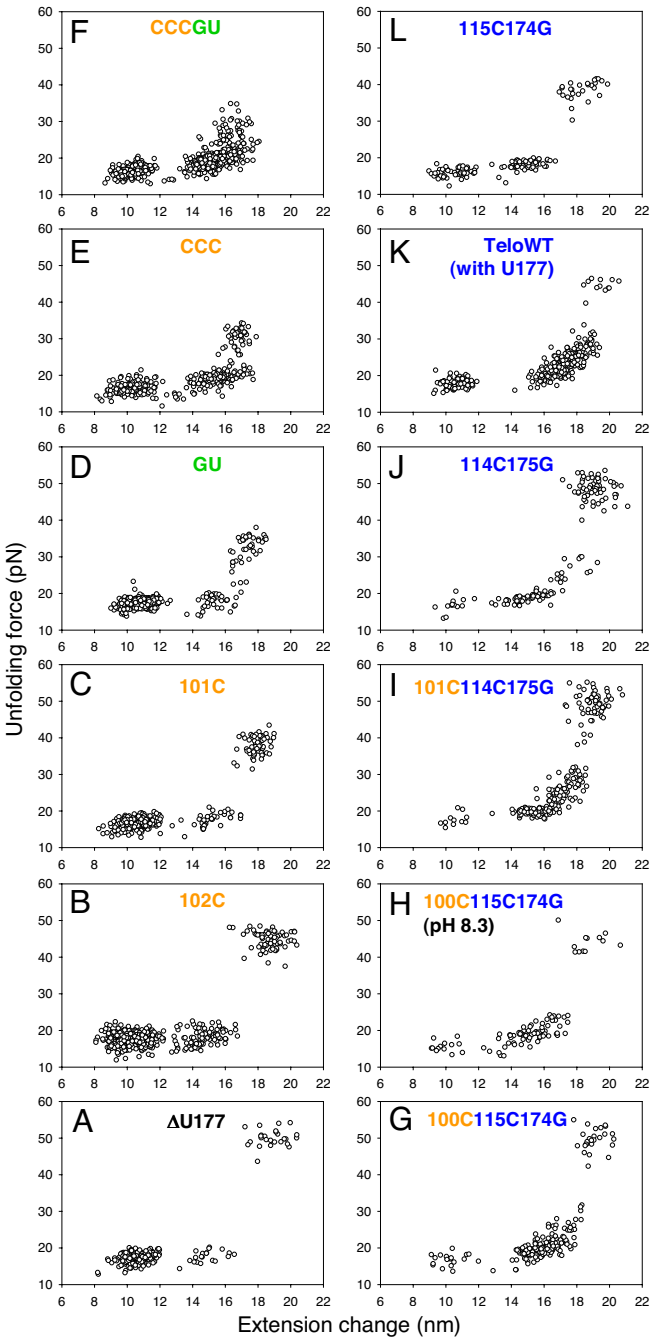

Fig. S3. Summary of results obtained for all pseudoknots. All pseudoknot mutants were made based on ΔU177. Plots of unfolding force versus extension change reveal 3 classes of unfolding reactions. Shown on bottom left of each plot are the second steps of low-force 2-step unfolding reactions. Shown on bottom right and top right of each plot are low-force 1-step and high-force 1-step unfolding reactions, respectively. All of the unfolding forces were measured at pH 7.3 except for mutant 100C115C174G, which was also measured at pH 8.3 (see *H*).

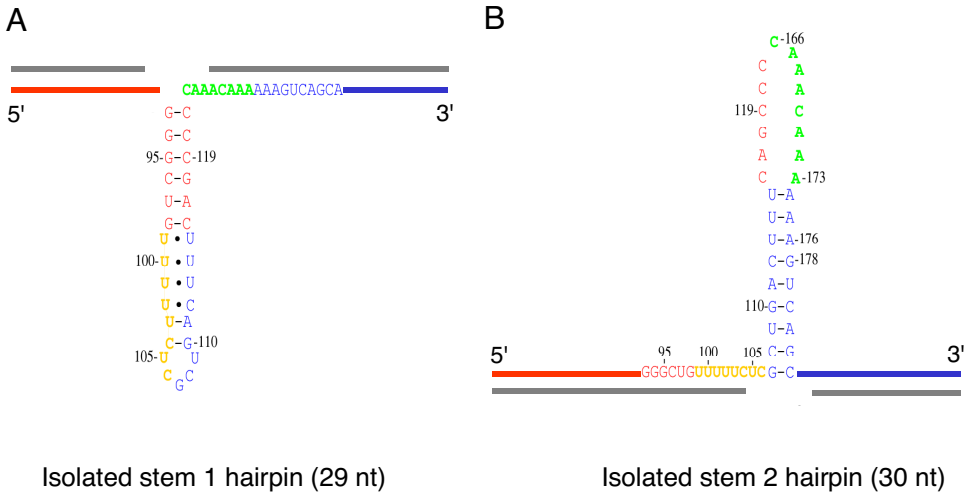

Fig. S4. Constructs of isolated stem 1 hairpin and isolated stem 2 hairpin. (*A*) Isolated stem 1 hairpin derived from pseudoknot ΔU177 is made by extended RNA/DNA handle to hybridize the 3′ parts of ΔU177. (*B*) Isolated stem 2 hairpin derived from pseudoknot ΔU177 is made by extended RNA/DNA handle to hybridize the 5′ parts of ΔU177.

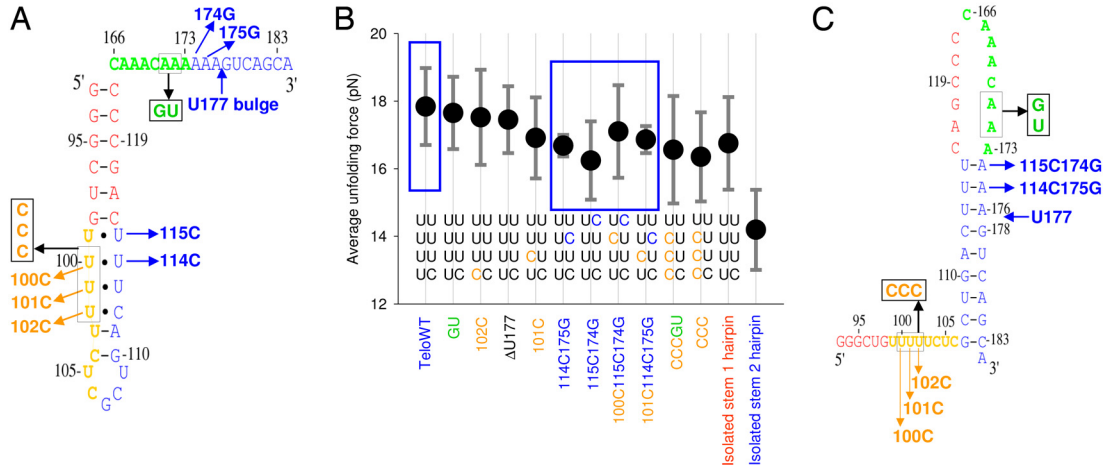

Fig. S5. Effect of mutation on unfolding forces of stem 1 hairpin. (*A*) Secondary structures of stem 1 hairpins derived from pseudoknot ΔU177 and mutants. In addition to Watson-Crick U-A and C-G pairs, 3 U·U and 1 U·C pairs are formed in the loop of 6-bp stem 1 hairpin as shown by an NMR structure (1). A U·U pair has 2 hydrogen bonds and is usually thermodynamically more stable than a U·C or C·C pair (2, 3). Mutations in loop 1 and stem 2 are expected to change the stability of the stem 1 hairpin. (*B*) Average unfolding forces for the second step of pseudoknot unfolding. Formation of non-Watson-Crick C·C, C·U, and U·C pairs upon mutations in loop 1 and stem 2 is indicated. Average unfolding forces for isolated stem 1 and isolated stem 2 hairpin derived from pseudoknot ΔU177 (see Fig. S4) are shown for comparison. Error bars are standard deviations from Gaussian fits. The second step unfolding forces for the pseudoknots without mutations in stem 2 roughly correlate with the number of U·U pairs remaining in the loop of stem 1 hairpin. Shown in blue squares are pseudoknots with mutations in stem 2. The U-A to C-G mutation in stem 2 stabilizes partially formed stem 2 in the folding intermediate (see Fig. 3*B*) and destabilizes stem 1 hairpin (see *A*), resulting in increased first step unfolding force (see Fig. S6*E* for example) and decreased second step unfolding force, respectively. Thus, less clear trends were observed for the second step unfolding forces for pseudoknots with mutations in stem 2 (shown in the larger blue squares). The average unfolding force of the isolated stem 2 hairpin from ΔU177 is at least 2 pN lower than those of the second step unfolding for all 11 pseudoknots, suggesting that the second step of pseudoknot unfolding corresponds to unfolding of stem 1 hairpin. Mutation of 1 U-A to C-G adjacent to the loop of 9-bp stem 2 hairpin is unlikely to increase the unfolding force by 2 pN, because the mutated base pairs adjacent to the loop (see *C*) are still formed at the mechanical unfolding transition state. Thus, stem 1 hairpin forms before stem 2 for all of the pseudoknots studied here (see Fig. 3). (*C*) Secondary structures of stem 2 hairpins derived from pseudoknot ΔU177 and mutants.

1. Theimer CA, Finger LD, Trantirek L, Feigon J (2003) Mutations linked to dyskeratosis congenita cause changes in the structural equilibrium in telomerase RNA. *Proc Natl Acad Sci USA* 100:449–454.
2. Mathews DH, Disney MD, Childs JL, Schroeder SJ, Zuker M, Turner DH (2004) Incorporating chemical modification constraints into a dynamic programming algorithm for prediction of RNA secondary structure. *Proc Natl Acad Sci USA* 101:7287–7292.
3. Mathews DH, Sabina J, Zuker M, Turner DH (1999) Expanded sequence dependence of thermodynamic parameters improves prediction of RNA secondary structure. *J Mol Biol* 288:911–940.

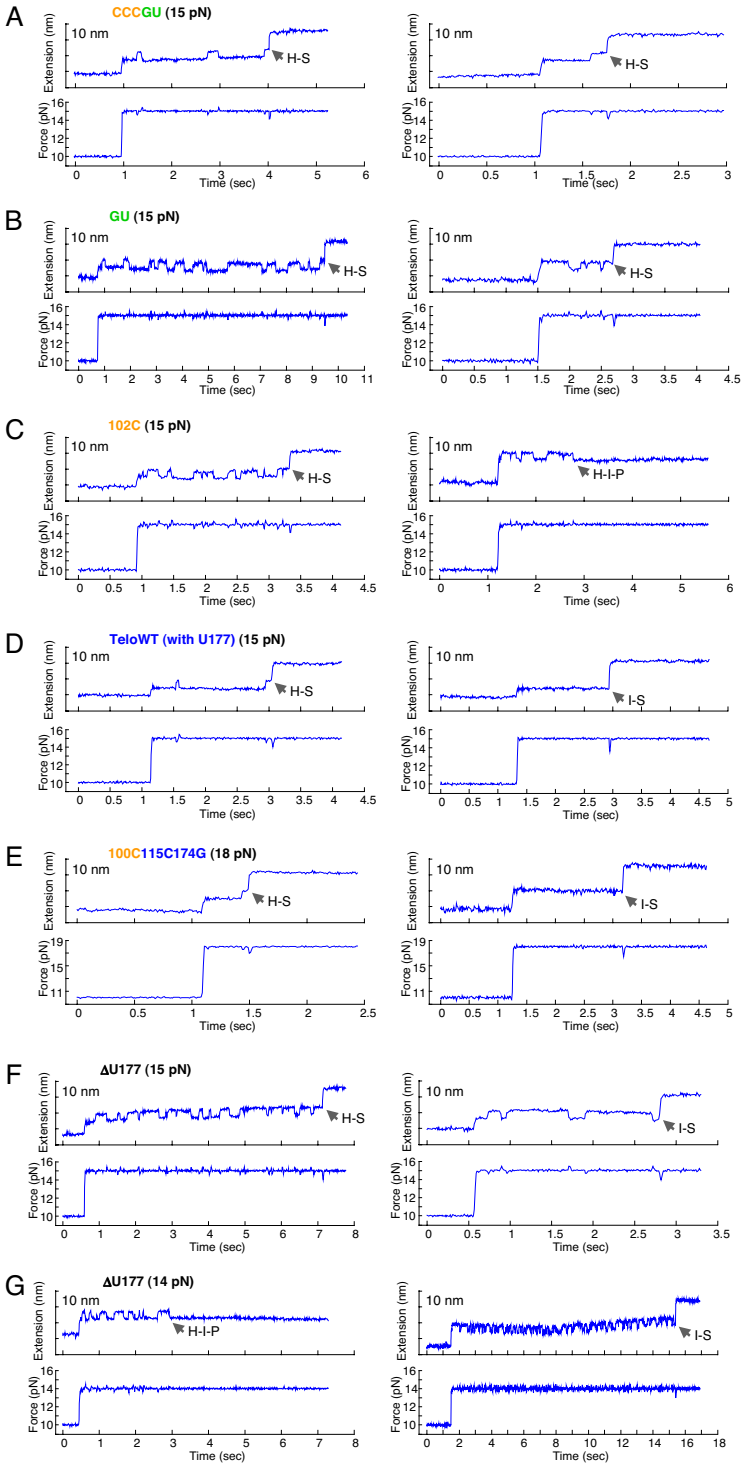

Fig. S6. Representative force-jump trajectories for several pseudoknots. Force was jumped from 10 pN to 14, 15, or 18 pN and maintained constant by force feedback. Unfolding of folding intermediates (I, see Fig. 3) in 1 step or 2 steps was observed. In 2-step unfolding reactions, the partially formed stem 2 unfolds first (I-H, with extension increase of approximately 5 nm) followed by unfolding of stem 1 hairpin to single strand (H-S, with extension increase of ≈11 nm). Hopping is observed with the rates depending on the stability of stem 1 hairpin and folding intermediate. In most trajectories, hopping suddenly stopped due to unfolding of stem 1 hairpin to single strand (H-S, with extension increases of ≈11 nm) or unfolding of folding intermediate to single strand (I-S, with extension increase of ≈15 nm). Stem 1 hairpin folds typically below 10 pN. Hopping may also stop less frequently due to formation of native pseudoknot [H-I-P, see right trace in *C* (mutant 102C), left trace in *G* (ΔU177), and trace 1 in Fig. S2*G*]. Note that there is no observable extension change for the I-P transition because the folding intermediate and native pseudoknot have similar molecular extensions (Fig. 3*B* and *C*). Native pseudoknot structures of ΔU177 and mutant 102C unfolds above 35 pN.

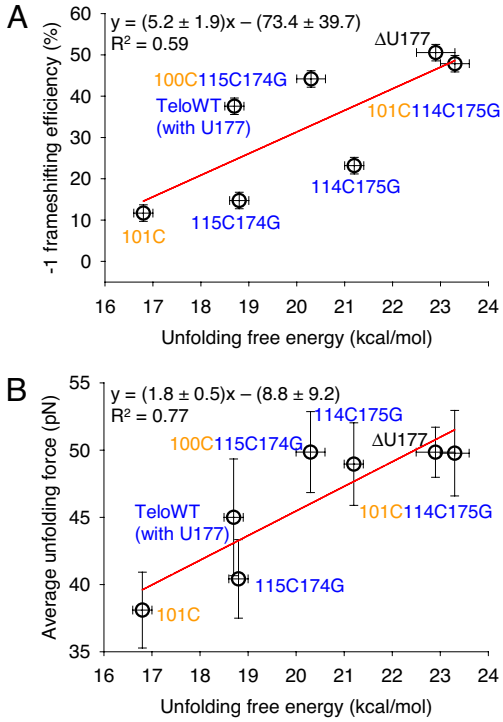

Fig. S7. Native pseudoknot unfolding free energy, native pseudoknot average unfolding force, and FS efficiency. All pseudoknot mutants were made based on ΔU177. The free energies of ΔU177 and TeloWT were previously measured by bulk thermal unfolding in 1 M NaCl at pH 7 and 37 °C (1). NMR structures reveal that 5 base triples are formed in TeloWT, although TeloWT is destabilized relative to ΔU177 by 4.2 kcal/mol (≈29 pN·nm) in free energy (all free energies mentioned in this paper are at 37 °C) (1, 2). Consistently, TeloWT unfolds at 45 pN with FS efficiency of approximately 40%. Five of the pseudoknot mutants studied here differ from those studied by thermal unfolding by only the U177 bulge. For these molecules we subtracted the free energy increment of 4.2 kcal/mol due to the U177 bulge (1, 3) to facilitate comparison between the native pseudoknot free energy, average unfolding forces, and FS efficiency. Error bars for unfolding force are standard deviations from Gaussian fits. Error bars for free energy and FS efficiency are standard deviations of bulk measurements. (*A*) Plot of FS versus unfolding free energy. There is weak correlation ($R^2 = 0.59$) between FS efficiency and unfolding free energy. (*B*) Plot of average unfolding force versus unfolding free energy. The unfolding forces (in 200 mM NaCl at pH 7.3 and 22 °C) roughly correlate with unfolding free energies (in 1 M NaCl at pH 7 and 37 °C). It seems that the unfolding force reaches a plateau at approximately 50 pN with an unfolding free energy above 20 kcal/mol. Note that a U·G-C base triple with 1 hydrogen bond in the Hoogsteen U·G pair may be formed in both mutant 115C174G and mutant 114C175G (Fig. S1*C*). Thus, mutations have similar thermodynamic effect on mechanical unfolding transition states and native pseudoknot structures, implying that the triplex structures are still formed at the mechanical unfolding transition state. We did not obtain the force-dependent unfolding kinetics from unfolding force distributions because of the presence of multiple unfolding pathways (4). It is likely that TeloWT mechanical unfolding is initiated by partial breaking of stem 2 while mutant 115C174G, 100C115C174G, 114C175G, and 101C114C175G have stem 1 partially broken at the mechanical unfolding transition state.

1. Theimer CA, Blois CA, Feigon J (2005) Structure of the human telomerase RNA pseudoknot reveals conserved tertiary interactions essential for function. *Mol Cell* 17:671–682.
2. Kim NK, et al. (2008) Solution structure and dynamics of the wild-type pseudoknot of human telomerase RNA. *J Mol Biol* 384:1249–1261.
3. Mathews DH, Sabina J, Zuker M, Turner DH (1999) Expanded sequence dependence of thermodynamic parameters improves prediction of RNA secondary structure. *J Mol Biol* 288:911–940.
4. Dudko OK, Hummer G, Szabo A (2008) Theory, analysis, and interpretation of single-molecule force spectroscopy experiments. *Proc Natl Acad Sci USA* 105:15755–15760.

Table S1. Summary of results obtained for all molecules. All pseudoknot mutants were made based on ΔU177

Pseudoknot	Folding waiting time at 3 pN (s)	Total pairs of beads	Total number of tethers	Total number of traces	Total numbers and percentages of three classes of unfolding reactions		
					Low-force 2-step	Low-force 1-step	High-force 1-step
CCCGU	0 or 10	9	13	560	148 (26%)	412 (74%)	
CCC	0 or 10	6	9	361	173 (48%)	188 (52%)	
GU	10	8	12	364	282 (77%)	82 (23%)	
101C	10	4	7	391	296 (76%)	36 (9%)	59 (15%)
102C	0	6	11	761	594 (78%)	99 (13%)	68 (9%)
ΔU177	0 or 10	10	13	247	201 (81%)	20 (8%)	26 (11%)
115C174G	10	5	8	150	58 (39%)	65 (43%)	27 (18%)
TeloWT (with U177)	10	9	13	321	94 (29%)	215 (67%)	12 (4%)
114C175G	10	6	8	148	14 (9%)	72 (49%)	62 (42%)
101C114C175G	10	8	10	237	11 (5%)	167 (70%)	59 (25%)
100C115C174G (pH 8.3)	10	1	2	96	14 (15%)	70 (73%)	12 (12%)
100C115C174G	10	8	9	211	19 (9%)	166 (79%)	26 (12%)

Test experiments for several pseudoknots suggest that the unfolding force distributions do not change significantly upon varying the lowest folding force (e.g., 0.5, 1, and 5 pN) and the waiting time (e.g., 20 and 30 s). The first trace of a newly established single-molecule tether between a new pair of beads was observed to always have high-force 1-step unfolding. After the first high-force 1-step unfolding event, low-force 1-step or 2-step unfolding events were more frequent. Molecular tethers broke very often with forces above 30 pN mainly due to the rupture of digoxigenin-antidigoxigenin interaction. Preformed structures in stem 1 hairpin decrease the kinetics of complete formation of stem 2 (see Fig. 3) (1). The single-molecule results are also consistent with slow kinetics observed for intramolecular DNA triplex formation in bulk experiments (2).

1. Wyatt JR, Puglisi JD, Tinoco I, Jr (1990) RNA pseudoknots: Stability and loop size requirements. *J Mol Biol* 214:455–470.
2. Roberts RW, Crothers DM (1996) Kinetic discrimination in the folding of intramolecular triple helices. *J Mol Biol* 260:135–146.